Journal of Power Sources 205 (2012) 495–499

Contents lists available at SciVerse ScienceDirect

Journal of Power Sources

journal homepage: www.elsevier.com/locate/jpowsour

Short communication

Mesoporous carbon–Cr_2O_3 composite as an anode material for lithium ion batteries

Bingkun Guo[a], Miaofang Chi[b], Xiao-Guang Sun[a,*], Sheng Dai[a,c,*]

[a] Chemical Sciences Division, Oak Ridge National Laboratory, Oak Ridge, TN 37831, USA
[b] Materials Science & Technology Division, Oak Ridge National Laboratory, Oak Ridge, TN 37831, USA
[c] Department of Chemistry, University of Tennessee, Knoxville, TN 37996, USA

ARTICLE INFO

Article history:
Received 12 December 2011
Received in revised form 10 January 2012
Accepted 12 January 2012
Available online 21 January 2012

Keywords:
Mesoporous carbon
Chromium oxide
Conversion reaction
Lithium ion battery

ABSTRACT

Mesoporous carbon–Cr_2O_3 (M-C–Cr_2O_3) composite was prepared by co-assembly of *in situ* formed phenolic resin, chromium precursor, and Pluronic block copolymer under acidic conditions, followed by carbonization at 750 °C under Argon. The TEM results confirmed that the Cr_2O_3 nanoparticles, ranging from 10 to 20 nm, were well dispersed in the matrix of mesoporous carbon. The composite exhibited an initial reversible capacity of 710 mAh g^{-1} and good cycling stability, which is mainly due to the synergic effects of carbons within the composites, i.e. confining the crystal growth of Cr_2O_3 during the high temperature treatment step and buffering the volume change of Cr_2O_3 during the cycling step. This composite material is a promising anode material for lithium ion batteries.

Published by Elsevier B.V.

1. Introduction

To date, Li-ion batteries are dominant in the portable electronic market as power sources owing to their advantages in voltage and energy densities as compared with other battery technologies [1–3]. However, cost, safety, service life, as well as limited energy density and power capability have limited their massive application in electric vehicles (EVs). To further increase the energy density of lithium ion batteries, many high capacity electrode materials have been explored [1–3]. As a distinctive family, transition metal oxides, such as Co_3O_4 [4,5], MnO [6], Fe_3O_4 [7] and CuO [8] have also been explored due to their attractive capacities as high as 700–1000 mAh g^{-1}. Among the transition-metal oxides, Cr_2O_3 has been considered as a promising anode material for lithium ion batteries because of its high theoretical capacity of 1058 mAh g^{-1} and relatively low emf value of 1.085 V [9]. However, as commonly observed on other transition metal oxides [7,10], bulk Cr_2O_3 materials usually suffer from poor cycling stability due to significant volume change and aggregation of the pulverized and/or nanosized particles, and thus hinder their practical applications in lithium ion batteries. It has been reported that using a nanostructured approach or synthesizing active materials with mesoporous structures could effectively improve the cycling stability of Cr_2O_3 based lithium ion batteries [10–12]. For example, Tarascon et al. [11,12] synthesized mesoporous Cr_2O_3 as anode for lithium ion batteries, which exhibited better cycling performance than that of bulk Cr_2O_3. Unfortunately, the capacity based on Cr_2O_3 was only 300–400 mAh g^{-1}, which is much lower than the theoretical capacity of Cr_2O_3.

An alternative strategy to increase the capacity and improve cycling performance of Cr_2O_3 is to form a composite with another material, which can restrain the volume change of Cr_2O_3 during cycling. Carbon has been routinely used for this purpose to form composite with active materials displaying large volumetric changes during cycling such as Si [13] and Sn [14,15], and as a result, the composites all exhibited better electrochemical performance than those of the pristine materials. However, the carbon materials used in the above cases could not well buffer the volume change because of their nonporous nature. To well accommodate the volume change, mesoporous carbon would be a better choice. Recently, we have demonstrated that mesoporous carbons could easily be synthesized via a soft-template approach, which exhibited not only a high lithium storage capacity of 1000 mAh g^{-1} but also good rate capabilities [16]. Another advantage of using mesoporous carbon is that its capacity and electrochemical activity range are similar to those of Cr_2O_3 and therefore the capacity of the composite will not be compromised. Here, we report an *in situ* synthesis of composite anode material consisting of mesoporous carbon and Cr_2O_3 (M-C–Cr_2O_3) using a soft-template approach, which shows high capacity and excellent cycling stability.

* Corresponding authors. Tel.: +1 865 241 8822; fax: +1 865 576 5235.
E-mail addresses: sunx@ornl.gov (X.-G. Sun), dais@ornl.gov (S. Dai).

0378-7753/$ – see front matter. Published by Elsevier B.V.
doi:10.1016/j.jpowsour.2012.01.092

2. Experimental

M-C–Cr_2O_3 was prepared by carbonization of a polymeric composite, which was obtained by self-assembly of *in situ* formed phenolic resin and Pluronic block copolymer under an acidic condition [17–20]. Briefly, 2.2 g of resorcinol ($C_6H_6O_2$, Sigma–Aldrich) and 2.2 g of F127 ($EO_{106}PO_{70}EO_{106}$, Aldrich) were dissolved in a mixed solution of 9 ml EtOH and 9 ml HCl (3 M). To this solution, 2.6 g of formaldehyde (37%) was then added. After stirring for about 30 min at room temperature, the polymer-rich gel phase was collected after centrifugation at 8500 rpm for 6 min. The gel phase and 7.86 g chromium nitrate ($Cr(NO_3)_3{\cdot}9H_2O$, Aldrich) were well mixed in 20 ml ETOH and poured on a petri dish, dried overnight, and then cured in an oven at 80 °C for 24 h. Carbonization was carried out under Argon atmosphere at 400 °C for 2 h with a heating rate of 1 °C min^{-1}, followed by treatment at 750 °C for 6 h with a heating rate of 5 °C min^{-1}. For comparison, Cr_2O_3 was prepared by sintering chromium nitrate ($Cr(NO_3)_3{\cdot}9H_2O$) under the same condition as that for M-C–Cr_2O_3. In addition, mesoporous carbon was also prepared under the same condition, and labeled as MC-750.

Nitrogen adsorption isotherms were measured at −196 °C using TriStar 3000 volumetric adsorption analyzer manufactured by Micromeritics Instrument Corp. (Norcross, GA). Before adsorption measurements the carbon powders were degassed in flowing nitrogen for 1–2 h at 200 °C. The specific surface area of the samples was calculated using the Brunauer–Emmett–Teller (BET) method within the relative pressure range of 0.05–0.20. TEM and EELS analysis were carried out on a FEI Titan 60/300 (S)TEM microscope equipped with a Gatan Image Filter (GIF) Quantum. The electrodes were rinsed with dimethyl carbonate (DMC) in an argon-filled glove box and dried in a vacuum chamber. Afterwards, they were dispersed on lacey carbon grids and loaded on a TEM vacuum transfer holder in a glove box to eliminate air-exposure. Each EELS spectrum was acquired from a "fresh" area under 300 kV without pre-e-beam exposure. The energy shift of each core-loss spectrum was carefully calibrated by using a corresponding zero loss peak (ZLP) which was acquired simultaneously using Gatanduol-EELS system.

Wide-angle X-ray diffraction (WAXS) patterns were recorded on a Siemens D5005 diffractometer operating at 40 kV and 40 mA. The thermal gravimetric analysis (TGA) profile was recorded on a TGA thermogravimetric analyser (TA Instruments, Inc.) under air environment. Electrochemical experiments were carried out by using coin cells. The working electrode was prepared by mixing M-C–Cr_2O_3, carbon black and poly(vinylidenedifluoride), PVDF, at a weight ratio of 80:10:10. The slurry was casted on Cu foil and dried under an infrared lamp to remove the solvent, followed by drying in a vacuum oven at 100 °C for 12 h. The loading of active materials is between 1.0 and 2.0 mg cm^{-2}. Celgard 2320 was used as separator and lithium foil was used as both counter and reference electrode. The electrolyte consisted of a solution of 1 M $LiPF_6$ in ethylene carbonate (EC)/dimethyl carbonate (DMC)/diethyl carbonate (DEC) (1:1:1 by volume). The carbonates and $LiPF_6$ were all obtained from Novolyte Corporation. The cells were assembled in an argon-filled glove box with moisture and oxygen level below 0.5 ppm. Galvanostatic discharge–charge experiments were tested in the voltage range of 0.005–3.0 V on an Arbin battery test system.

3. Results and discussion

So far, most of reported mesoporous materials were prepared by inverse replicas of ordered mesoporous silica templates (hard-templating method) [21,22], which required tedious steps such as synthesis of the silica templates, impregnation of the silica pores with a precursor and the use of toxic chemicals such as hydrofluoric acid (HF) or sodium hydroxide (NaOH) to etch the silica templates after sintering. As a contrast, the mesoporous composite M-C–Cr_2O_3 was prepared by soft template approach via self-assembly of *in situ* formed phenolic resin and Pluronic block copolymer under acidic condition [18,19]. Both Cr precursor and copolymer template can be well dispersed in EtOH to form a homogeneous gel. After sintering at 750 °C under Ar atmosphere, the Cr precursor was decomposed *in situ* to form M-C–Cr_2O_3.

Fig. 1a displays the WAXS patterns of the synthesized M-C–Cr_2O_3 and Cr_2O_3 samples. All recorded peaks can be ascribed to those of Cr_2O_3 (JCPDS: 06-0504) and no Cr or other chromium oxides peaks were detected, suggesting that pure Cr_2O_3 was obtained even after high-temperature treatment in the presence of carbon. In order to confirm the content of carbon in the M-C–Cr_2O_3 composite, thermal gravimetric analysis (TGA) under air environment was used. As shown in Fig. 1b that the M-C–Cr_2O_3 composite contains 42% carbon and 58% Cr_2O_3.

The N_2 adsorption–desorption isotherms and corresponding pore size distribution curves for M-C–Cr_2O_3 are shown in Fig. 1c and d, respectively. M-C–Cr_2O_3 sample exhibits a typical type IV nitrogen adsorption/desorption isotherm with a pronounced uptake in the relative pressure range (P/P_0) of 0.4–0.7, indicating uniform mesoporous structure. The pore width in the PSD curves (Fig. 1d) is about 4.5 nm and the BET surface area is 505 $m^2\ g^{-1}$.

Fig. 2 shows the typical TEM images of M-C–Cr_2O_3 and Cr_2O_3. Different from previous reports of ordered structure [17–20], the M-C–Cr_2O_3 sample shows disordered mesoporous structure, which might be due to the high Cr_2O_3 content in the composite (58 wt%). The dark spots in the low magnification images (Fig. 2a and b) are Cr_2O_3 nanoparticles, which are homogeneously dispersed in the carbon matrix. The crystal Cr_2O_3 nanoparticles within the M-C–Cr_2O_3 composite, ranging from 10 to 20 nm, can be easily observed in the high magnification image (Fig. 2c). As a comparison, the particle size of Cr_2O_3 shown in Fig. 2d is not homogeneous with diameter ranging from tens to hundreds nanometer. The smaller and homogeneous particle in M-C–Cr_2O_3 indicates that the carbon within the composite effectively suppressed the Cr_2O_3 particle growth and agglomeration during the high temperature treatment.

Fig. 3a shows the CV curves for the M-C–Cr_2O_3 electrode at a scan rate of 0.1 mV s^{-1} in the voltage range of 0.0–3.0 V. In the cathodic scan there is a pronounced reduction peak between 0.85 and 0.13 V. The reduction peak is the result of the electrolyte decomposition and concomitant solid electrolyte interphase (SEI) formation, which is mainly observed during the first cycle and almost disappeared in the following cycles. In the anodic scan one broad oxidation peak is observed between 0.6 and 1.6 V. No obvious oxidation peak for Cr is observed, which could be ascribed to the nanoparticle size and/or the amorphous natures of the production after conversion reactions of the transition-metal oxides [11,12].

The lithium storage property of the M-C–Cr_2O_3 sample was evaluated by galvanostatic discharge–charge tests at a current density of 50 mA g^{-1}. For comparison, Cr_2O_3 and MC-750 were also evaluated under the same condition. The discharge (Li uptake)/charge (Li removal) profiles for the M-C–Cr_2O_3 electrode are shown in Fig. 3b. The reversible capacity based on the total weight of M-C–Cr_2O_3 composite is 710 mAh g^{-1}, which is more than two times the reversible capacity of commercial graphite (350 mAh g^{-1}). The reversible capacity of mesoprous carbon MC-750, as shown in Fig. 3c, is 700 mAh g^{-1}. Therefore, the calculated reversible capacity of Cr_2O_3 within the composite is only 717 mAh g^{-1} $((710 - 700 \times 0.42)/0.58)$. This capacity is much lower than the theoretical capacity of Cr_2O_3 (1058 mAh g^{-1}), which might be directly related to the fact, as suggested by Tarascon et al. [11,12], that during the charge process chromium monoxide (CrO) rather than Cr_2O_3 was formed. To verify this, the cell charged to 3 V after initial discharge to 0 V was disassembled inside the glove box and the electrode was washed with dry dimethyl carbonate (DMC).

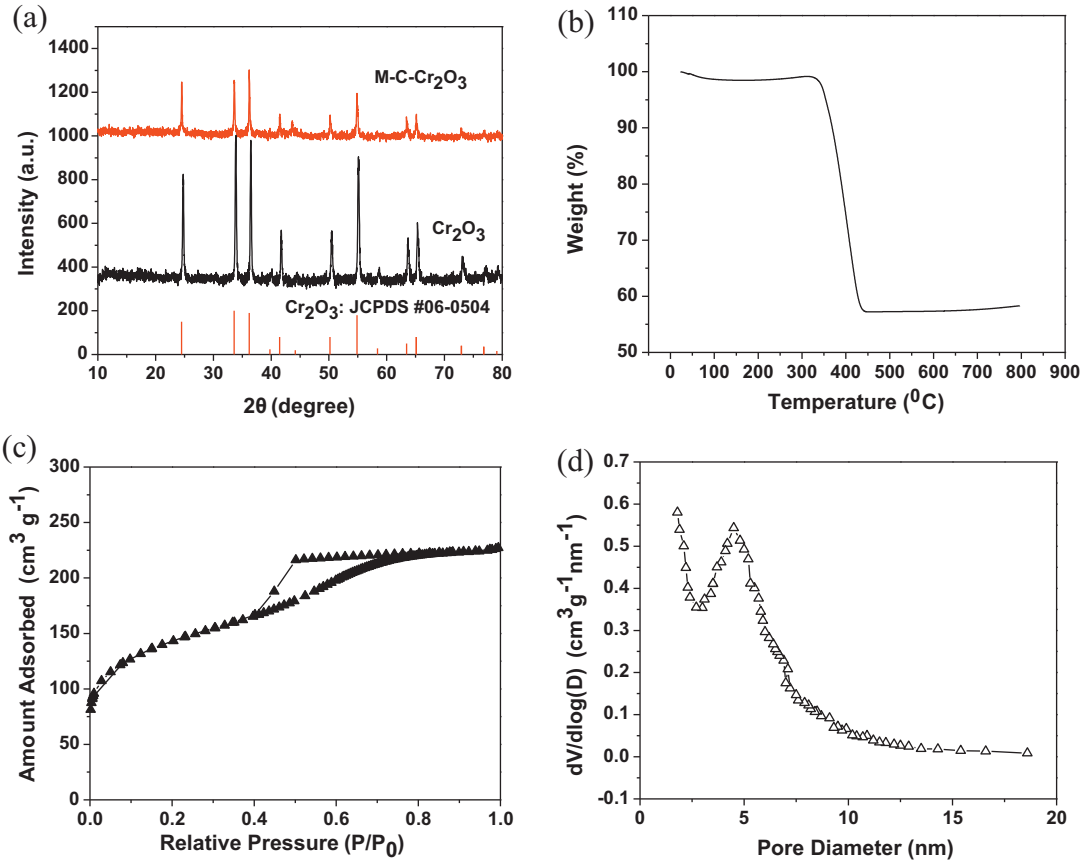

Fig. 1. WAXS (a) and TGA (b) of M-C–Cr_2O_3; nitrogen adsorption isotherms (c) and BJH pore size distribution plots (d) for M-C–Cr_2O_3.

After it was dried in the antechamber of the glove box, some powder was scraped off the electrode for TEM/EELS study. As shown in Fig. 3d that the Cr-L spectrum from the charged sample is shifted toward lower energy compared to that of the pristine Cr_2O_3 sample, indicating that indeed Cr in the charged product has a lower oxidation state than 3^+ as in Cr_2O_3. Also, the drop of O-K pre-peak (at ~529 eV), which can be assigned to unoccupied oxygen 2p orbitals hybridized with the chromium 3d orbitals, confirms

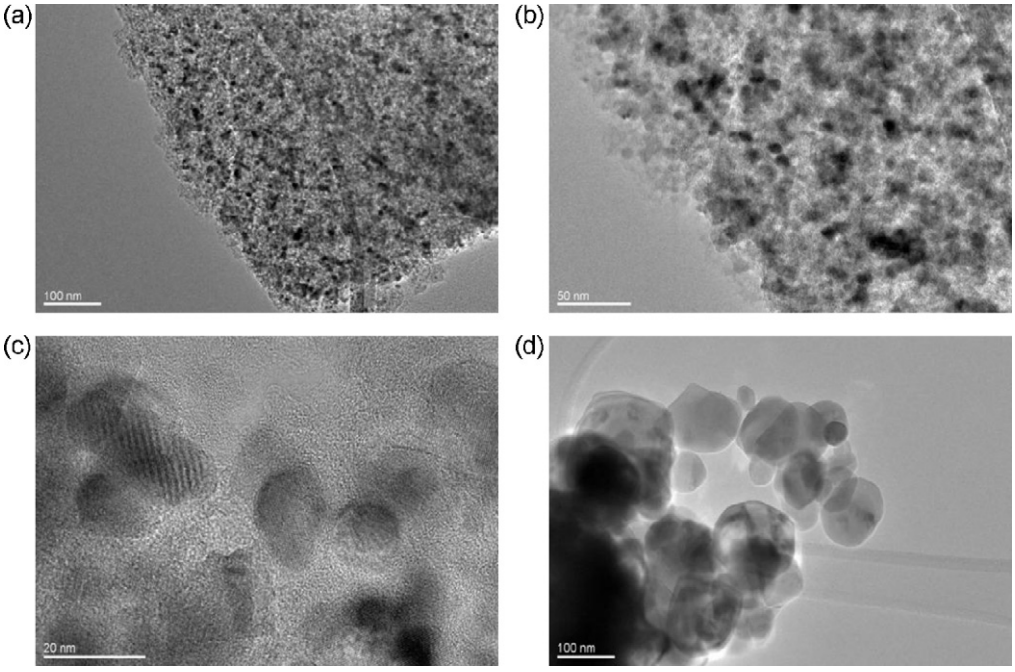

Fig. 2. Typical TEM images of M-C–Cr_2O_3 (a, b, c) and Cr_2O_3 (d).

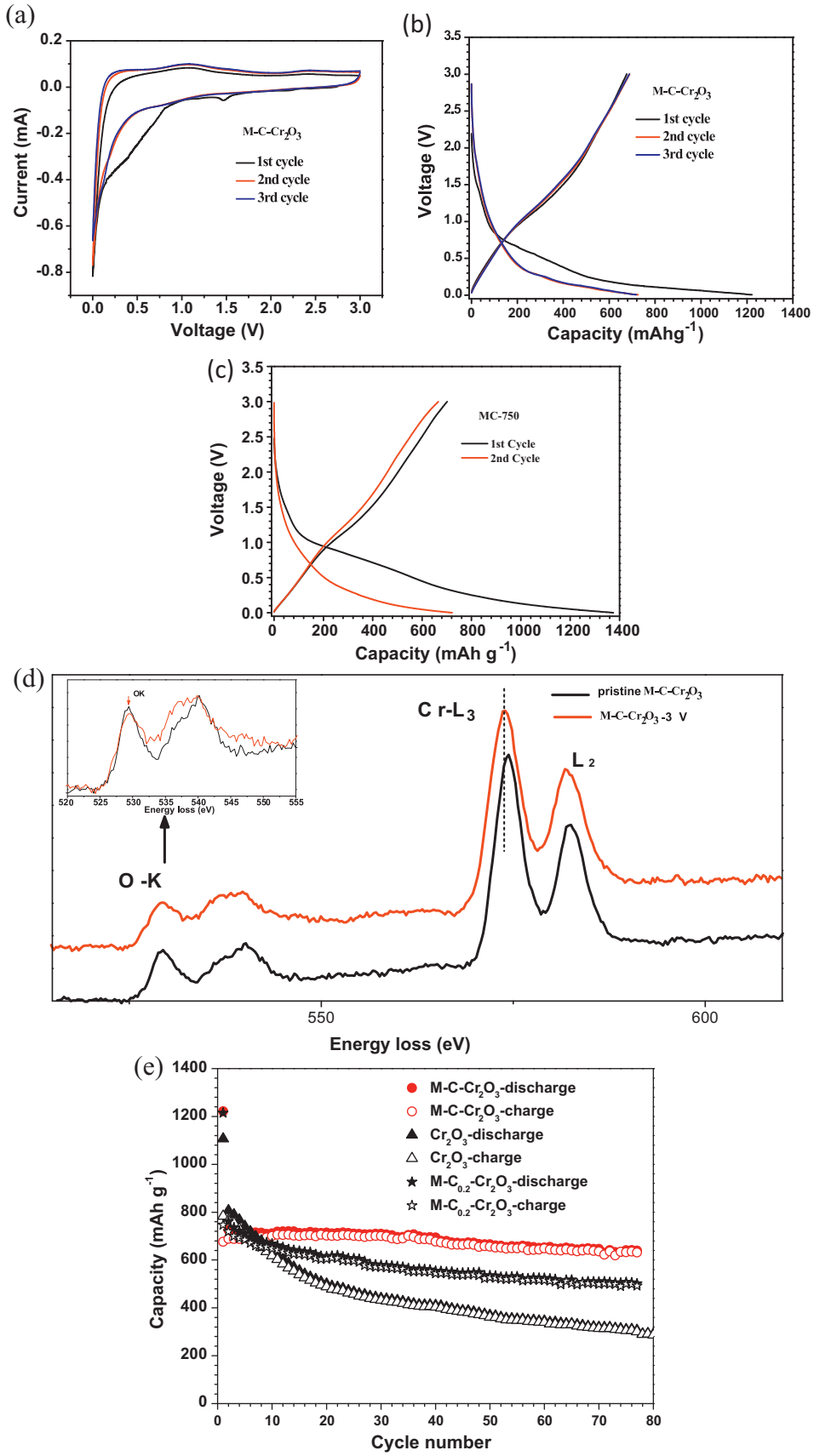

Fig. 3. (a) Cyclic voltammograms of M-C–Cr_2O_3 at a scan rate of 0.1 mV s^{-1} in the voltage range of 0.0–3.0 V; (b) galvanostatic discharge (Li uptake, voltage decreases)/charge (Li removal, voltage increases) curves of M-C–Cr_2O_3 and (c) MC-750 electrodes at a current density of 50 mA g^{-1}; (d) EELS comparison of the pristine M-C–Cr_2O_3 and the recharged M-C–Cr_2O_3 sample (3.0 V) (each spectrum shown here is an average of 40 spectra from eight different grains); (e) cycle performance comparison between Cr_2O_3, M-C–Cr_2O_3 and M-$C_{0.2}$–Cr_2O_3 under the current density of 50 mA g^{-1}.

that the valence states of the Cr element in the recharged sample and that in the pristine sample are different. These spectra evidence confirms that the charged product might contain significant amount of CrO rather than pure Cr_2O_3 [23–25]. Furthermore, the observation that the nominal reversible capacity of 717 mAh g^{-1} for the Cr_2O_3 within the composite being close to the theoretical capacity of CrO (744 mAh g^{-1}) also supports the above conclusions.

It is also noted, as often observed for other mesoporous materials [26,27], that the initial irreversible capacity of M-C–Cr_2O_3 is very large (545 mAh g^{-1}), resulting in an initial coulombic efficiency of 55%. However, after the first few cycles, the coulombic efficiency quickly improves above 98%. The large initial irreversible capacity may come from two sources. One source is due to the large specific surface area (505 m^2 g^{-1}), which results in the electrolyte decomposition and the SEI formation during the discharge process [28,29]. The other source is due to the fact that the charged product contains significant amount of CrO rather than Cr_2O_3, which results in a lower charge capacity. In the following cycles, Cr and CrO are cycled reversibly during the discharge and charge process, resulting in higher coulombic efficiencies.

Fig. 3e compares the cycling performance of the cells based on M-C–Cr_2O_3 and Cr_2O_3 electrodes. The Cr_2O_3 cell capacity decays rapidly with cycling whereas the M-C–Cr_2O_3 cell not only exhibits a high reversible capacity but also excellent cycling stability. After 80 cycles the reversible capacity of the M-C–Cr_2O_3 cell is still as high as 639 mAh g^{-1}, which is much better than that previously reported performance of nanostructure Cr_2O_3 or C–Cr_2O_3 composite [30,31]. The poor performance of Cr_2O_3 cell, as mentioned before, is due to the significant volume variation and the aggregation of the pulverized particles during repeated charge/discharge process [10]. The significantly enhanced performance of the M-C–Cr_2O_3 cell is attributed to the presence of carbon and its mesoporous structure. First, as shown in Fig. 2 that carbon restrains the growth of Cr_2O_3 during the high-temperature treatment, which results in less volume change during discharge/charge process and improves the cycling performance. Secondly, mesoporous carbon acts as a buffer for volume change during the Li uptake/removal, providing enough structural stability for the electrode and culminating in its better cycling stability as compared with pure bulky Cr_2O_3. Finally, the carbon in the composite increases the electronic conductivity of the composite.

It should be emphasized that the first two carbon effects within the composite are more important than the last one in improving the cycling performance. For the sake of improving electronic conductivity 20% of carbon or even less should be enough, however, it might not be enough to improve the cycling performance. This is evident in the performance comparison of the composite with 20% carbon versus that with 40% carbon. As shown in Fig. 3e that under the same condition the capacity of the composite with 20 wt% of carbon (M-$C_{0.2}$–Cr_2O_3) decreases quickly within the first 20 cycles, after which it slowly decreases. Obviously, the cycling stability of the composite with 20% carbon is much worse than that of the composite with 40% carbon, even though it is much better than the bare Cr_2O_3 materials. The above fact indicates that 20% carbon might not be enough in restraining the crystal growth of Cr_2O_3 during the high temperature treatment process and preventing capacity decay during the cycling process. Nevertheless, the high capacity and good cycling performance of M-C–Cr_2O_3 make it a good candidate as anode for application in lithium ion batteries.

4. Conclusion

The carbon–Cr_2O_3 composite was easily synthesized by an *in situ* soft-template approach at 750 °C. The composite exhibited much better cell performance than the bulk Cr_2O_3 under the same cycling condition. The improved performance is mainly due to the synergic effects of carbons, i.e. confining the crystal growth of Cr_2O_3 during the high temperature treatment step and buffering the volume change of Cr_2O_3 during the cycling step. The favorable electrochemical properties combined with the advantages of the soft-templating approach to prepare M-C–Cr_2O_3 nanocomposites make these materials good anode candidates for lithium ion batteries.

Acknowledgements

The main part of this work was supported by the U.S. Department of Energy's Office of Basic Energy Science, Division of Materials Sciences and Engineering, under contract with UT Battelle, LLC. B.K.G. was supported by the DOE VT program. M.F.C. would like to thank the support of ORNL's SHaRE User Facility, which is sponsored by the DOE Office of Basic Energy Science.

References

[1] Y. Idota, T. Kubota, A. Matsufuji, Y. Maekawa, T. Miyasaka, Science 276 (1997) 1395.
[2] P. Poizot, S. Laruelle, S. Grugeon, L. Dupont, J.M. Tarascon, Nature 407 (2000) 496.
[3] H. Li, X.J. Huang, L.Q. Chen, Z.G. Wu, Y. Liang, Electrochemical and Solid State Letters 2 (1999) 547.
[4] V. Pralong, J.B. Leriche, B. Beaudoin, E. Naudin, M. Morcrette, J.M. Tarascon, Solid State Ionics 166 (2004) 295.
[5] K.T. Nam, D.W. Kim, P.J. Yoo, C.Y. Chiang, N. Meethong, P.T. Hammond, Y.M. Chiang, A.M. Belcher, Science 312 (2006) 885.
[6] K.F. Zhong, X. Xia, B. Zhang, H. Li, Z.X. Wang, L.Q. Chen, Journal of Power Sources 195 (2010) 3300.
[7] L. Taberna, S. Mitra, P. Poizot, P. Simon, J.M. Tarascon, Nature Materials 5 (2006) 567.
[8] X.P. Gao, J.L. Bao, G.L. Pan, H.Y. Zhu, P.X. Huang, F. Wu, D.Y. Song, Journal of Physical Chemistry B 108 (2004) 5547.
[9] H. Li, P. Balaya, J. Maier, Journal of the Electrochemical Society 151 (2004) A1878.
[10] P.G. Bruce, B. Scrosati, J.M. Tarascon, Angewandte Chemie – International Edition 47 (2008) 2930.
[11] L. Dupont, S. Grugeon, S. Laruelle, J.M. Tarascon, Journal of Power Sources 164 (2007) 839.
[12] L. Dupont, S. Laruelle, S. Grugeon, C. Dickinson, W. Zhou, J.M. Tarascon, Journal of Power Sources 175 (2008) 502.
[13] Y.S. Hu, R. Demir-Cakan, M.M. Titirici, J.O. Muller, R. Schlogl, M. Antonietti, J. Maier, Angewandte Chemie – International Edition 47 (2008) 1645.
[14] G. Derrien, J. Hassoun, S. Panero, B. Scrosati, Advanced Materials 19 (2007) 2336.
[15] B.K. Guo, J. Shu, K. Tang, Y. Bai, Z.X. Wang, L.Q. Chen, Journal of Power Sources 177 (2008) 205.
[16] B.K. Guo, X.Q. Wang, P.F. Fulvio, M.F. Chi, S.M. Mahurin, X.G. Sun, S. Dai, Advanced Materials 23 (2011) 4661.
[17] C.D. Liang, S. Dai, Journal of the American Chemical Society 128 (2006) 5316.
[18] X.Q. Wang, C.D. Liang, S. Dai, Langmuir 24 (2008) 7500.
[19] X.Q. Wang, S. Dai, Adsorption – Journal of the International Adsorption Society 15 (2009) 138.
[20] C.D. Liang, Z.J. Li, S. Dai, Angewandte Chemie – International Edition 47 (2008) 3696.
[21] R. Ryoo, S.H. Joo, M. Kruk, M. Jaroniec, Advanced Materials 13 (2001) 677.
[22] S. Jun, S.H. Joo, R. Ryoo, M. Kruk, M. Jaroniec, Z. Liu, T. Ohsuna, O. Terasaki, Journal of the American Chemical Society 122 (2000) 10712.
[23] M.F. Chi, N. Browning, N. Orlovskaya, Journal of Solid State Electrochemistry 10 (2006) 659.
[24] A.M. Arevalo-Lopez, M.A. Alario-Franco, Inorganic Chemistry 48 (2009) 11843.
[25] T.L. Daulton, B.J. Little, Ultramicroscopy 106 (2006) 561.
[26] Y.S. Hu, P. Adelhelm, B.M. Smarsly, S. Hore, M. Antonietti, J. Maier, Advanced Functional Materials 17 (2007) 1873.
[27] H.S. Zhou, S.M. Zhu, M. Hibino, I. Honma, M. Ichihara, Advanced Materials 15 (2003) 2107.
[28] Z.X. Wang, X.J. Huang, R.J. Xue, L.Q. Chen, Carbon 37 (1999) 685.
[29] B.K. Guo, N. Liu, J.Y. Liu, H.J. Shi, Z.X. Wang, L.Q. Chen, Electrochemical and Solid State Letters 10 (2007) A118.
[30] J. Hu, H. Li, X.J. Huang, L.Q. Chen, Solid State Ionics 177 (2006) 2791.
[31] L.Y. Jiang, S. Xin, X.L. Wu, H. Li, Y.G. Guo, L.J. Wan, Journal of Materials Chemistry 20 (2010) 7565.